CBS COPENHAGEN BUSINESS SCHOOL
HANDELSHØJSKOLEN

How do different forecasting models and training segments compare in predicting the average number of three-point shots made by NBA teams per game?

Predictive Analytics (CDSCO1005E)

Student: Johannes Stärk

Pages: 10

Characters (with Space): 22.283

Date: June 13, 2025

Copenhagen Business School
Department of Digitalization
2000 Frederiksberg
rg.digi@cbs.dk

Contents

1 Introduction

Since its introduction in the 1979–80 season, the three-point shot has evolved from an experimental tactic to a vital component of the NBA, significantly impacting offensive strategies and player roles. Teams that once emphasized interior post play now prioritize spacing and long-range shooting, while traditional centers have been compelled to develop perimeter skills to remain effective. This evolution is evident in the increase from fewer than one three-point shot per game in 1980 to an average of more than 12 per game by 2022, reflecting a broader shift in basketball philosophy and talent development (NBA, n.d.).
Therefore, forecasting the monthly average number of three-point shots made per team emerges as a timely and relevant challenge. Accurate prediction of these metrics can inform coaching decisions, roster construction and in-game strategy, enabling organizations to gain a competitive edge in a league where shooting proficiency is key. This report compares forecasting models and training segments, assessing their capacity to identify trends and structural changes, as well as the increasing significance of long-range shooting in the NBA.

2 Related Work

Time-series forecasting is widely used in sports analytics, including in the field of basketball. Several studies have used ARIMA models to predict performance metrics such as three-pointers, assists and overall scoring. For instance, McCollum used annual, league-wide NBA data from 1979 to 2019 to develop an ARIMA model that predicted an ongoing increase in three-point shooting, though at a decelerating rate. Other analyses have applied ARIMA to team or player data at the season level and demonstrated improved accuracy over naïve or mean-based forecasting methods (McCollum, 2019). In other domains, such as ice hockey, ARIMA has also been used to model player performance. Lambrix and Sysoev transformed NHL play-by-play data into a time series and applied ARIMA to detect trends. Interestingly, they found that simple models often fit best, suggesting minimal time-dependent structure in this context (Lambrix & Sysoev, 2019). While these studies demonstrate the applicability of ARIMA in sports forecasting, they exhibit important limitations. Most rely on coarse temporal resolution, such as season- or annual-level data, and typically assume a uniform structure across time. This makes it difficult to capture shifts in playing style, league dynamics or the effect of major rule changes. Additionally, few studies compare ARIMA to alternative model families, such as exponential smoothing (ETS), which may be more suitable for data with evolving levels and trends. This project addresses these limitations by using monthly, team-level data and applying rule-based segmentation to reflect structural changes in NBA history. Furthermore, it directly compares ARIMA with ETS models across these segments to evaluate which approach is more effective in different historical contexts.

3 Data Preprocessing & Exploration

To create a robust forecasting model for predicting NBA teams' three-point shooting performance, the data had to be preprocessed to make it easier to structure and aggregate, which was done in Python using Pandas. Initially, the raw data provided detailed statistics on individual player performances per game, which included significant variability and potential noise. Recognizing this, the data was aggregated monthly rather than at the level of individual games. The main reason for this was to reduce short-term variability, or 'noise', such as day-to-day fluctuations in player performance or opponent variability, which may not represent consistent patterns. Specifically, the preprocessing involved two critical aggregation steps:

1. **Game-Level Aggregation per Team:** The dataset was grouped by individual dates and teams. For each game, the average number of three-point shots made by each team was calculated, resulting in a single clear metric per team per game. This eliminated redundancy and clarified team-level performance.

2. **Monthly Aggregation Across All Teams:** Subsequently, these team-level daily averages were aggregated into monthly averages. This involved grouping the data by month and calculating the average three-point performance across all teams.

Applying this method consistently across all available seasons ensured uniformity and enabled broader, more stable patterns to be identified. This structured, noise-reduced dataset formed a solid basis for predicting the monthly average number of three-point shots made by NBA teams. Next off-season months and data from before the introduction of the three-point line, focusing on relevant and meaningful periods, were removed. Structural breaks resulting from major rule changes or eras shaped by players such as Stephen Curry were identified and modeled using dummy variables (Freitas, 2021). This enabled the model to explicitly account for shifts in gameplay trends and evolving playing styles driven by these pivotal changes.

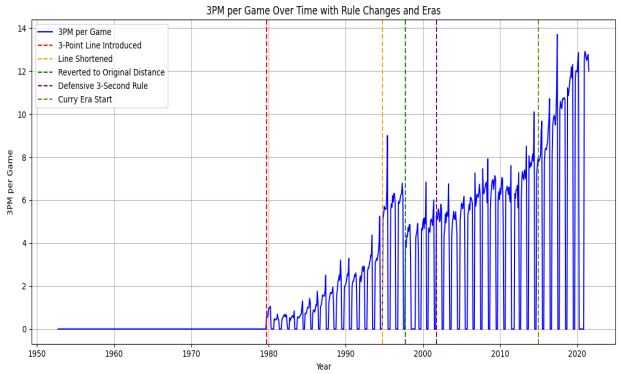

Figure 1: Preprocessed Time Series

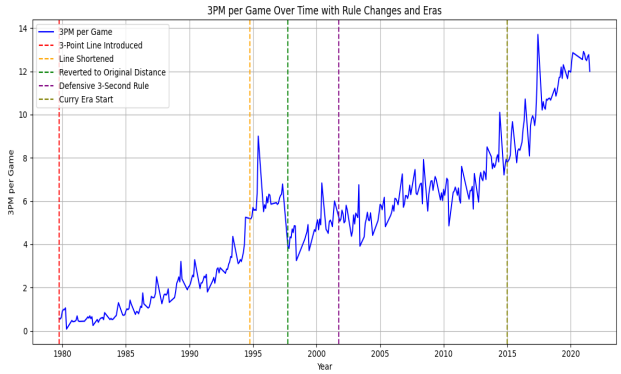

Figure 2: Preprocessed Time Series (Off-Season removed)

Although the STL decomposition of the three-point monthly average time series revealed a clear recurring cyclic component (see Figure 3), closer examination of the seasonal plots showed no consistent pattern within seasons across the years. Overlays of individual seasons failed to align with any characteristic monthly behavior, suggesting that the observed cycles largely arise from calendar effects rather than stable seasonal drivers (see Figure 4). Consequently, no seasonal adjustment was applied later in the process, enabling the model to focus solely on the underlying trend and structural shifts.

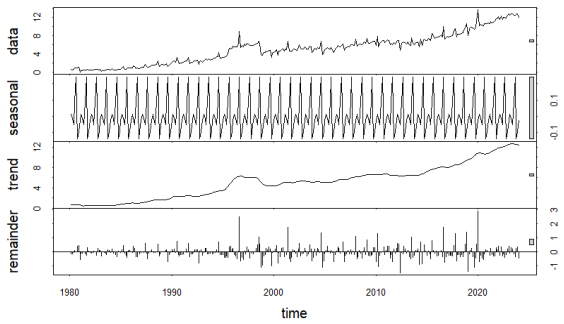

Figure 3: STL-Decomposition

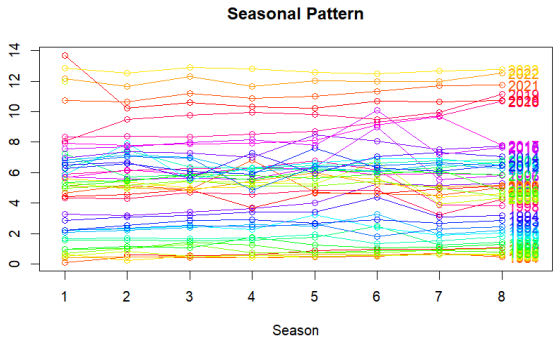

Figure 4: Seasonal Pattern

The final dataset comprises 352 monthly observations, corresponding to 44 NBA seasons (each with eight active months). The monthly average three-pointers made per game grew from approximately 0.7 at the start of the series to about 12.5 by the most recent month, reflecting an overall increase of nearly 11.8 three-pointers per game. This trajectory implies a compound annual growth rate in three-point attempts of roughly 7.3%, highlighting the steady rise in long-range shooting over the past four decades.

4 Methodology

This analysis uses a consistent forecasting methodology applied to different segments of the NBA dataset. To ensure comparability across models and time contexts, the minimum viable training period was defined as the Curry era (2015-2019). Based on this segment, an 80/20 train-test split was constructed, where the training set includes data up to September 2019 and the test set spans from October 2019 onwards.

The same train-test cut-off was then applied to the longer training segments, the modern era (1997-2019) and the full dataset (1979-2019), so that each model forecasts the same out-of-sample period. This design enables a fair comparison of forecasting performance across different historical contexts. A structured modeling pipeline was applied to each training segment: data transformation, stationarity testing using the Augmented Dickey-Fuller (ADF) test, differencing

if required, and model fitting using both ETS and ARIMA. While these preprocessing steps were necessary for ARIMA to meet its assumptions of stationarity and constant variance, ETS models were directly fitted to the original data, as they do not require prior transformation or stationarity. The following sections outline this methodology using the modern era as a running example; however, the same process was applied uniformly to all segments and model types.

4.1 Structural Breaks

The evolving nature of NBA gameplay was taken into account by identifying structural breaks and incorporating them into the modeling process. These breaks are defined as points at which the underlying data dynamics change. The analysis began with the application of the Quandt likelihood ratio (QLR) test, which uses F statistics to detect significant changes in regression parameters over time (Hyndman & Athanasopoulos, 2021). Based on the optimal model fit, as determined by the Bayesian Information Criterion (BIC), this statistical method identified breakpoints in June 1995, June 2006, and November 2012.

These results (see Figure 5 & 6) were then compared with key rule changes and contextual developments in NBA history. Notably, two of the mathematically identified breakpoints aligned well with the period when the three-point line was shortened (from 1994 to 1997) and with the beginning of the Curry era (around 2015). While the 2006 breakpoint did not directly correspond to a specific rule change, it may reflect gradual shifts in strategic preferences, particularly with regard to shot selection.

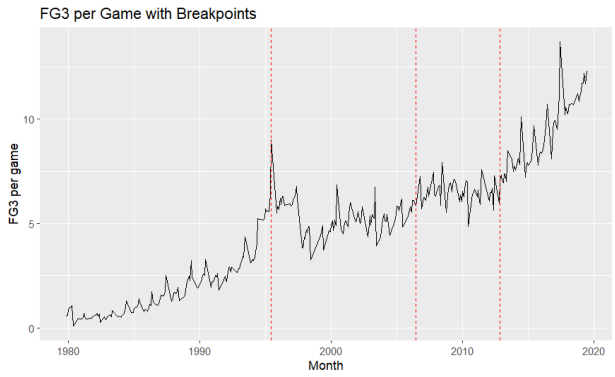

Figure 5: Plotted Statistical Structural Breaks

```
        Optimal (m+1)-segment partition:

Call:
breakpoints.formula(formula = Lag0 ~ Lag1, breaks = 3, data = fg3.tsi)

Breakpoints at observation number:

m = 1           273
m = 2       222 276
m = 3   132 222 276

Corresponding to breakdates:

m = 1                                        0.810089020771513
m = 2                       0.658753709198813 0.818991097922849
m = 3   0.391691394658754 0.658753709198813 0.818991097922849

Fit:

m   0     1     2     3
RSS 173.5 166.6 143.1 124.0
BIC 750.1 753.9 720.2 689.4
[1] "1995-06-01" "2006-06-01" "2012-11-01"
```

Figure 6: Statistical Structural Breaks in R

Due to the strong correspondence between the statistical evidence and the historical context, the analysis proceeded with the use of manually defined structural breaks. These defined segments were then used in subsequent modeling to enable the models to capture the unique trends of each period more accurately and improve forecasting performance by minimizing interference from unrelated historical shifts.

4.2 Mathematical Transformations

As described in the methodology introduction, mathematical transformations were applied to the datasets. These steps ensure that the data align with the assumptions of the subsequent models, which are detailed in Section 4.4 Model Selection. The transformations help to stabilize variance, reduce skewness and improve model fit (Hyndman & Athanasopoulos, 2021). Although logarithmic transformations are common, the Box–Cox transformation was chosen for its flexibility. Unlike a fixed log transformation, the Box–Cox method estimates an optimal parameter to adjust the transformation based on the characteristics of the data. This makes it especially effective at correcting heteroscedasticity and normalizing the data. Given the non-linear growth and varying variance in NBA three-point trends, the Box–Cox transformation was well suited to this analysis.

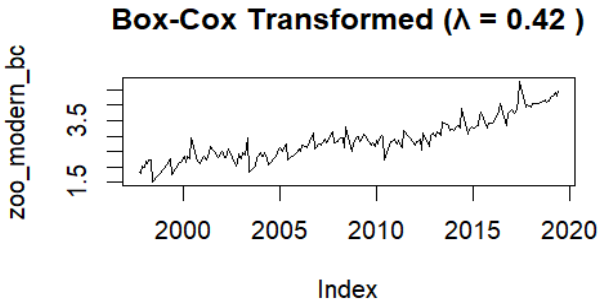

Figure 7: Box-Cox Transformed Modern Era

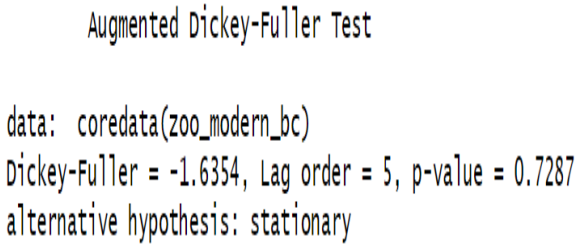

Figure 8: ADF for Transformed Modern Era

4.3 Stationarity & Differencing

In order to prepare the data for time series modeling, it was first necessary to establish whether it was stationary. A stationary time series has constant statistical properties, such as mean and variance, over time. Non-stationary data can lead to unreliable forecasts, particularly in models that assume temporal stability (Hyndman & Athanasopoulos, 2021).
The ADF test was applied to evaluate stationarity. This test determines whether a unit root is present in the data; the null hypothesis implies non-stationarity. If the ADF test indicated non-stationarity, first-order differencing was applied. This involves subtracting each value in the time series from its preceding value. This transformation removes trends and stabilizes the mean over time. After differencing, the ADF test was repeated to verify that the series was now stationary. This process was applied consistently to the entire time series, each structural segment and their combinations, ensuring that all datasets used for ARIMA modeling met the necessary assumptions for effective and accurate forecasting.

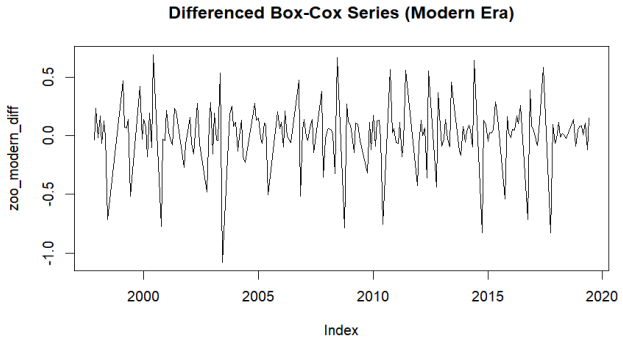

Figure 9: Differenced Modern Era

```
Augmented Dickey-Fuller Test

data:  coredata(na.omit(zoo_modern_diff))
Dickey-Fuller = -8.9041, Lag order = 5, p-value = 0.01
alternative hypothesis: stationary
```

Figure 10: ADF for Differenced Modern Era

4.4 Model Selection

Both ETS and ARIMA have their own advantages and reflect a different forecasting philosophy. The ETS (Error, Trend, Seasonality) model was chosen as a baseline due to its simplicity and adaptability. It naturally handles non-stationary data and captures changes in level and trend without the need for transformation. This makes it a strong candidate for short-term forecasting tasks and a useful benchmark.

The ARIMA (AutoRegressive Integrated Moving Average) model was selected for its robust treatment of temporal dependence and its ability to explicitly model autocorrelation and trend. To ensure a fair comparison, ARIMA models were also applied to each training segment used in the ETS model.

Applying both models to different structural training segments allows this framework to explore in detail how model type and historical context influence forecasting behavior and suitability.

5 Model Specifications

5.1 ETS

ETS models were fitted to each data segment and combination of segments identified in the preceding chapters. Across all subsets, the selected model was ETS(M, A, N), which consists of a multiplicative error term and an additive trend but no seasonal component. This specification was chosen consistently based on the structure and characteristics of the data.

The multiplicative error component (M) is appropriate because the variability in the series increases with its level. This pattern can be seen in the historical trend of NBA three-point shooting, where both the average number of successful shots and the variability have increased

over time. As the data were modeled in their original units, without log or Box-Cox transformation, a multiplicative error term is a suitable choice.
The additive trend component (A) reflects the series' steady upward movement. This is particularly evident in the modern era and the Curry era, where the increase in three-point shooting has been significant but not exponential. Therefore, an additive trend is more appropriate than a damped or multiplicative trend.
The absence of seasonality (N) is justified by the structure of the dataset. As the data is aggregated monthly, filtered to in-season games and averaged across teams, short-term seasonal effects are likely to be minimized. This is supported by earlier Seasonal Pattern Analysis, which revealed no strong or consistent seasonal patterns. After fitting each ETS model, residual diagnostics were performed to check for any remaining systematic patterns. ACF plots and the Ljung-Box test were used to assess whether the residuals behaved like white noise. For the Curry and Modern era models, the results showed no significant autocorrelation and the Ljung-Box test confirmed an adequate model fit. However, the full data model showed evidence of residual autocorrelation at higher lags, suggesting that some minor structures remained unexplained. Full diagnostics, including plots and test statistics, are provided in the Appendix.
Overall, the ETS(M, A, N) configuration provides a logical and statistically appropriate model for three-point shooting trends across all historical segments.

5.2 ARIMA

To demonstrate the ARIMA model specification process, we will continue to use the modern era segment as a running example. The input series was Box–Cox transformed to stabilize the variance, as previously described, and then passed to the ARIMA model, which determined the necessary differencing internally.
Autocorrelation (ACF) and partial autocorrelation (PACF) plots were created from the transformed and differenced series to guide manual specification of model parameters (Figure 11). The ACF plot showed a significant spike at lag 1, indicating the need for a moving average (MA) term. The PACF showed notable declines after lag 4, suggesting the inclusion of an autoregressive (AR) component of a similar order. Based on these patterns, ARIMA(4,1,1) and ARIMA(5,1,1) were selected as candidate models.
Additionally, the `auto.arima()` function was employed to automatically select an optimal model, using AIC and BIC as the selection criteria. All model variants for the modern era included a drift term. Although differencing usually eliminates linear trends, the Box–Cox transformed series exhibited a gradual upward tendency, which supports the use of a drift term to capture residual trend behavior. Notably, for the Curry-only segment, the final `auto.arima()` model did not include a drift term, reflecting the limited data horizon and potentially weaker trend signal over that shorter period.

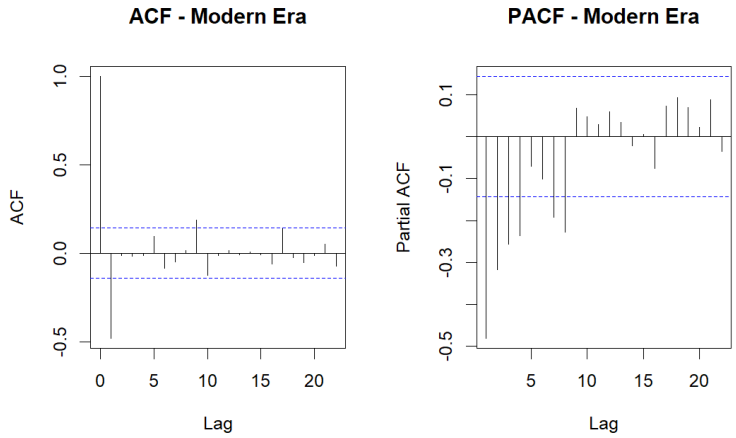

Figure 11: ACF & PACF for Transformed and Differenced Modern Ers Series

Each model was evaluated using the Akaike Information Criterion (AIC) and the Bayesian Information Criterion (BIC), both of which balance model fit with complexity. The table below summarizes the results:

Model	**Sigma**	**Log-Likelihood**	**AIC**	**BIC**
ARIMA(4,1,1) with Drift	0.211	28.27	-42.54	-19.9
ARIMA(5,1,1) with Drift	0.211	28.29	-40.6	-17.7
Auto ARIMA (0,1,1) with Drift	0.1163	138.01	**-270.03**	**-260.31**

Table 1: ARIMA Model Comparison on Modern Era Segment

This model selection procedure was applied consistently across all segments. In each case, the `auto.arima()` function selected the model with the lowest AIC and BIC, and this specification was used in the forecast comparison. Automated selection offers a data-driven and objective approach, reducing the risk of subjective overfitting and ensuring optimal balance between model complexity and fit. Interestingly, the selected model included no AR terms. This may be explained by the relatively weak and diffuse PACF pattern, which does not clearly support higher-order AR components. The algorithm therefore favored a more sparse model, relying instead on the moving average and drift components to capture the dynamics of the series.
After selecting the model, residual diagnostics were conducted to ensure suitability. The Ljung-Box test and ACF plots of residuals were used to check for autocorrelation. For the models selected via `auto.arima()` in each segment, the residuals largely resembled white noise, indicating that the models captured the underlying structure well. Minor autocorrelations were observed at isolated lags in the Curry and full dataset models, but these had minimal impact on overall performance. The `auto.arima()` models were therefore confirmed as the final specifications for all segments. Full residual plots and test statistics are provided in the Appendix.

6 Forecasts

Forecasts were generated using the final model for each data segment. To enable fair comparison of forecasting performance, the consistent test period was used across all experiments.

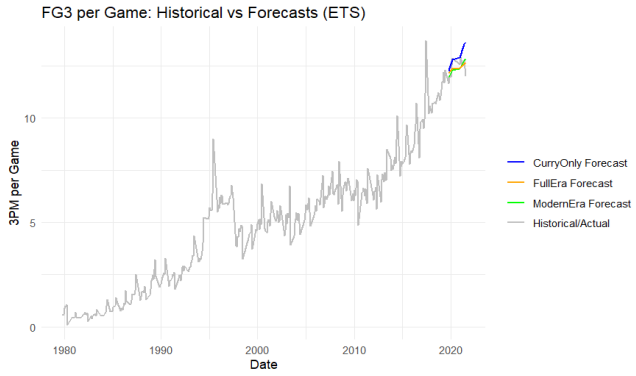

Figure 12: Forecasts with ETS

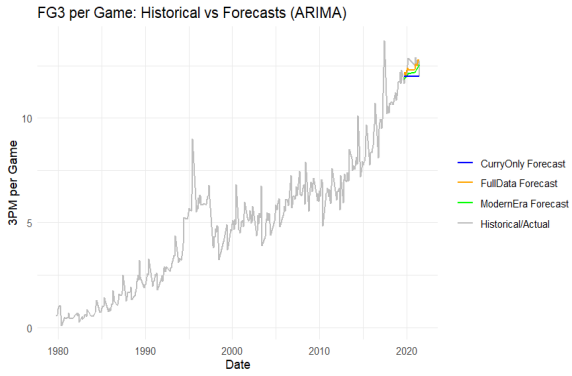

Figure 13: Forecasts with ARIMA

Four common evaluation metrics were used to assess forecast accuracy: RMSE, MAE, MAPE and MASE. Together, these metrics capture both absolute and relative prediction error, providing a comprehensive overview of model performance. The results in Table 2 show that models trained using the full dataset, as well as those from the modern era, generally performed better than models trained using only Curry-era data. For instance, in the ETS results, the model trained on the full dataset achieved the lowest RMSE (0.3372) and MAE (0.2841), with the model trained on data from the modern era achieving similar results (RMSE 0.3418, MAE 0.2448). By contrast, the Curry-only model produced noticeably higher error values (RMSE 0.6699, MAE 0.5475). These metrics offer different perspectives on forecast accuracy. RMSE (root mean square error) is sensitive to outliers because it gives greater weight to large errors, while MAE (mean absolute error) provides a straightforward average of the absolute differences between predicted and actual values. Lower values for both indicate better predictive performance. The higher error values in the Curry-only model may be due to the limited amount of training data available in that segment. With fewer observations and stronger short-term trends, the model may have overfitted recent fluctuations, reducing its ability to generalize. This pattern is even more evident in the ARIMA results. The full data ARIMA model produced an RMSE of 7.6711, whereas the Curry-only model performed substantially worse with an RMSE of 10.8438 and a very high MAPE of 87.2793. MAPE (mean absolute percentage error) measures the average error as a percentage of the actual values, making it useful for understanding the relative size of errors. The exceptionally high MAPE in the Curry-only model again suggests overfitting and poor generalization. In contrast, the modern-era ARIMA model performed better (RMSE 8.0032), likely because it captured recent trends while benefiting from a broader training window.

Metric	ETS			ARIMA		
	Curry-Only	Modern-Era	Full Data	Curry-Only	Modern-Era	Full Data
RMSE	0.6699	0.3418	0.3372	10.8438	8.0032	7.6711
MAE	0.5475	0.2448	0.2841	10.8368	7.9948	7.6626
MAPE	4.4548	1.9737	2.3016	87.2793	64.3707	61.6929
MASE	0.9259	0.4456	0.6520	464.0456	43.7381	38.9102

Table 2: Test Set Forecast Accuracy: ETS vs ARIMA Models

ETS models consistently outperformed ARIMA models across all segments. One likely reason for this is that ETS does not require the data to be stationary and can automatically adapt to changes in trend and level. By contrast, ARIMA relies heavily on differencing and proper transformation, both of which can be difficult to calibrate accurately, particularly when dealing with complex or short time series. Furthermore, ETS models tend to be more robust in the presence of noise or structural breaks in the data, which are common in sports analytics. Consequently, ETS provided more stable and accurate forecasts in this context.
Overall, the findings suggest that incorporating a broader historical context enhances forecast accuracy, and that ETS offers a more reliable and efficient modeling approach for predicting NBA three-point shooting trends.

7 Conclusion

The aim of this analysis was to answer the following question: How do different forecasting models and training segments compare in predicting the average number of three-point shots made by NBA teams per game? We evaluated the influence of model choice and training context on forecast accuracy by applying ETS and ARIMA models to different historical segments. The results showed that ETS outperformed ARIMA consistently across all configurations. Its flexibility and its ability to handle non-stationary data without transformation made it particularly effective. Interestingly, models trained on recent historical segments of sufficient length, particularly those from the modern era, achieved the highest accuracy. This suggests that including relevant past data while excluding outdated patterns may reduce noise and improve generalization.
In conclusion, the ETS model trained on the modern era segment produced the most accurate and reliable forecasts across multiple error metrics. This highlights the importance of selecting a flexible model and a well-balanced training window when forecasting dynamic trends in professional sports. Future work could incorporate player-level data or external factors, such as trades or injuries, or explore hybrid models to further enhance forecasting performance.

References

Freitas, L. (2021). Shot distribution in the NBA: Did we see when 3-point shots became popular? *German Journal of Exercise and Sport Research*, *51*(2), 237–240. https://doi.org/10.1007/s12662-020-00690-7

Hyndman, R. J., & Athanasopoulos, G. (2021). *Forecasting: Principles and practice* (Third print edition). Otexts, Online Open-Access Textbooks.

Lambrix, P., & Sysoev, O. (2019). Markov Decision Processes and ARIMA models to ana- lyze and predict Ice Hockey player's performance.

McCollum, E. (2019, December). Forecasting NBA Three Pointers Made for the Next Five Seasons | LinkedIn. Retrieved June 8, 2025, from https://www.linkedin.com/pulse/forecasting-nba-three-pointers-made-next-five-seasons-mccollum/

NBA. (n.d.). Players Traditional | Stats. Retrieved June 8, 2025, from https://www.nba.com/stats/players/traditional

Appendix

ETS

Fitted Models

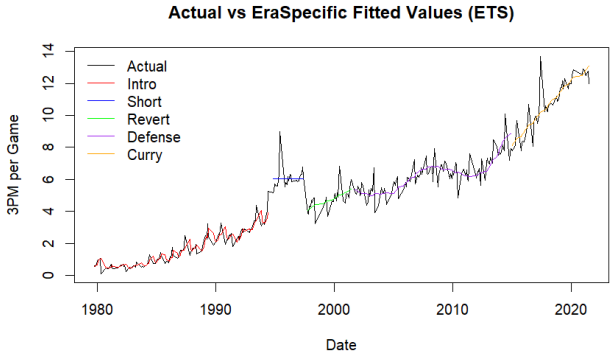

Figure 14: Fitted Models for each Era

Model Summaries

```
ETS(M,A,N)

Call:
ets(y = ts_curry_tr)

  Smoothing parameters:
    alpha = 1e-04
    beta  = 1e-04

  Initial states:
    l = 7.7613
    b = 0.1048

  sigma:  0.0782

     AIC     AICc      BIC
141.5743 143.2409 150.2626

Training set error measures:
                     ME      RMSE       MAE        MPE     MAPE      MASE      ACF1
Training set 0.002461842 0.7290583 0.4455625 -0.3710801 4.357973 0.4524557 0.1560093
```

Figure 15: Model Summary Curry-Only

```
ETS(M,Ad,N)

Call:
ets(y = ts_modern_tr)

  Smoothing parameters:
    alpha = 0.1936
    beta  = 0.004

  Initial states:
    l = 4.0595
    b = 0.0383

  sigma:  0.0974

     AIC     AICc      BIC
828.1300 828.4578 844.3387

Training set error measures:
                     ME      RMSE       MAE        MPE     MAPE      MASE         ACF1
Training set 0.04022262 0.6478077 0.4342483 -0.5471554 6.726107 0.6921737 -0.01300997
```

Figure 16: Model Summary Modern Era

```
ETS(M,A,N)

Call:
ets(y = ts_full_tr)

  Smoothing parameters:
    alpha = 0.6244
    beta  = 1e-04

  Initial states:
    l = 0.5474
    b = 0.0369

  sigma:  0.1537

     AIC     AICc      BIC
1579.078 1579.259 1598.193

Training set error measures:
                     ME      RMSE       MAE      MPE     MAPE      MASE       ACF1
Training set -0.003711682 0.6337517 0.3905392 -6.08777 14.17261 0.6668704 -0.1981411
```

Figure 17: Model Summary Full Data

Residuals

```
        Ljung-Box test

data:  Residuals from ETS(M,A,N)
Q* = 4.9583, df = 8, p-value = 0.762

Model df: 0.   Total lags used: 8


        Ljung-Box test

data:  Residuals from ETS(M,A,N)
Q* = 18.686, df = 16, p-value = 0.2853

Model df: 0.   Total lags used: 16


        Ljung-Box test

data:  Residuals from ETS(M,A,N)
Q* = 45.417, df = 16, p-value = 0.0001198

Model df: 0.   Total lags used: 16
```

Figure 18: Ljung-Box Test for Residuals for each Segment

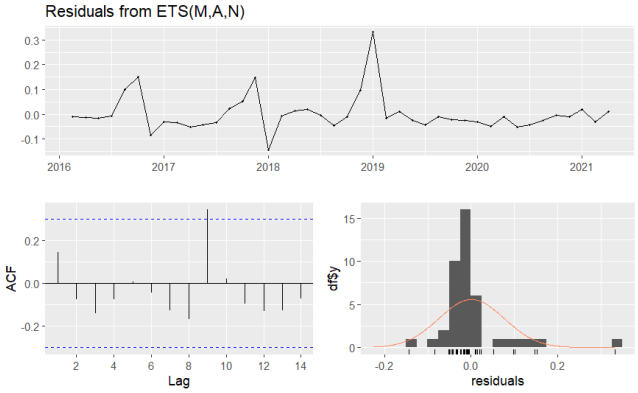

Figure 19: ETS Residuals for Curry-Only Segment

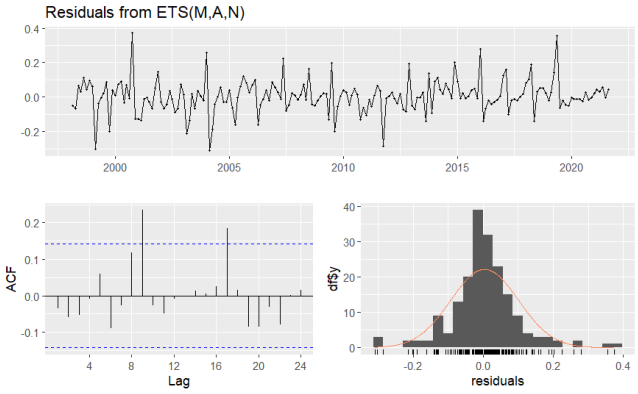

Figure 20: ETS Residuals for Modern-Era Segment

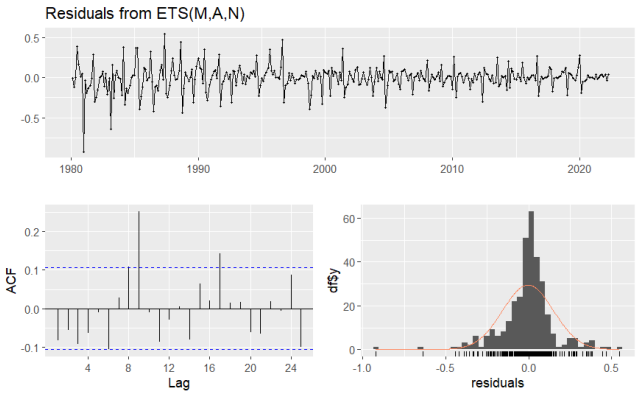

Figure 21: Combined ETS Fit across Segments

ARIMA

Transformation & Differencing Curry-Only

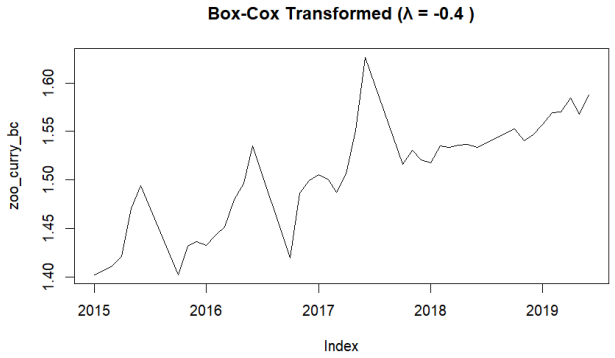

Figure 22: Box-Cox Transformed Curry Era

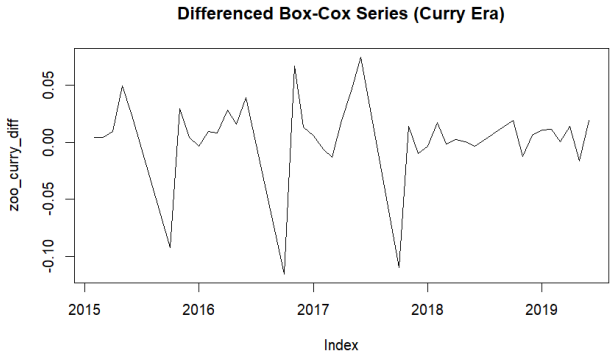

Figure 23: Box-Cox Transformed & Differenced Curry Era

```
        Augmented Dickey-Fuller Test

data:  coredata(zoo_curry_bc)
Dickey-Fuller = -3.3125, Lag order = 3, p-value = 0.08342
alternative hypothesis: stationary

Warning in adf.test(coredata(na.omit(zoo_curry_diff))) :
  p-value smaller than printed p-value

        Augmented Dickey-Fuller Test

data:  coredata(na.omit(zoo_curry_diff))
Dickey-Fuller = -5.2288, Lag order = 3, p-value = 0.01
alternative hypothesis: stationary
```

Figure 24: ADF Before and After Differencing

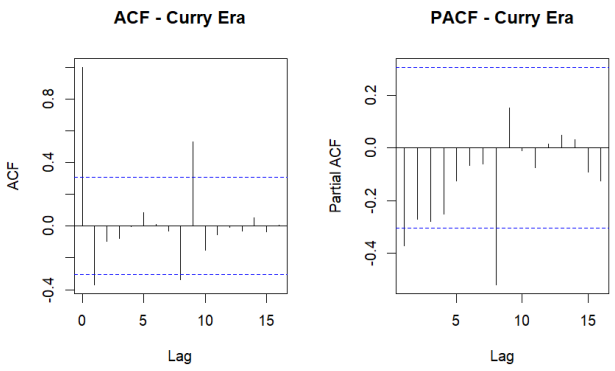

Figure 25: ACF & PACF of Transformed & Differenced Curry Era

Transformation & Differencing Modern-Era

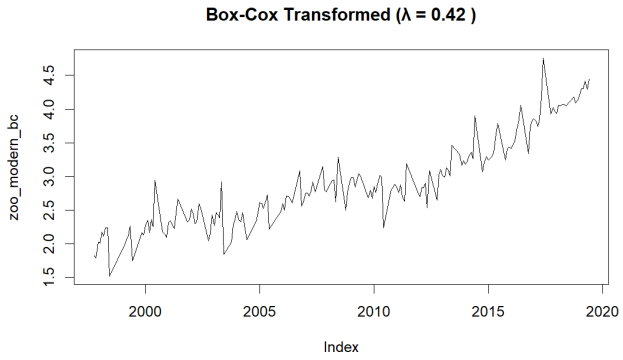

Figure 26: Box-Cox Transformed Modern Era

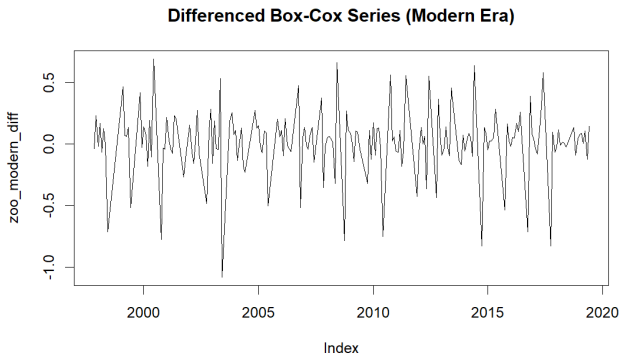

Figure 27: Box-Cox Transformed & Differenced Modern Era

```
        Augmented Dickey-Fuller Test

data:  coredata(zoo_modern_bc)
Dickey-Fuller = -1.6354, Lag order = 5, p-value = 0.7287
alternative hypothesis: stationary
```

```
Warning in adf.test(coredata(na.omit(zoo_modern_diff))) :
  p-value smaller than printed p-value
```

```
        Augmented Dickey-Fuller Test

data:  coredata(na.omit(zoo_modern_diff))
Dickey-Fuller = -8.9041, Lag order = 5, p-value = 0.01
alternative hypothesis: stationary
```

Figure 28: ADF Before and After Differencing

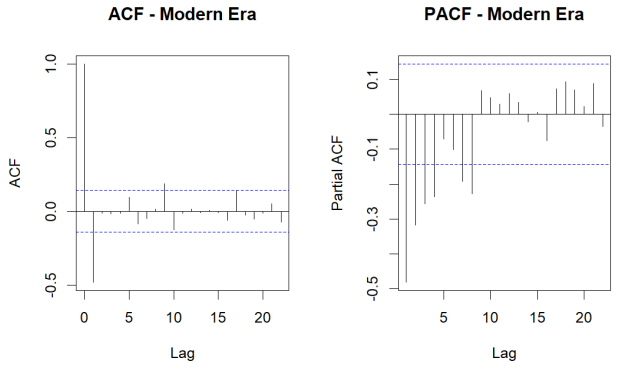

Figure 29: ACF & PACF of Transformed & Differenced Modern Era

Transformation & Differencing Full-Data

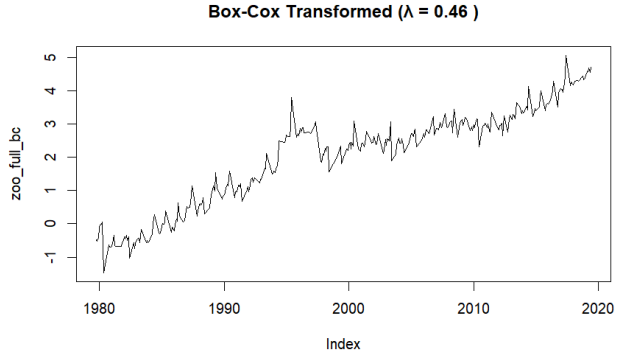

Figure 30: Box-Cox Transformed Full Data

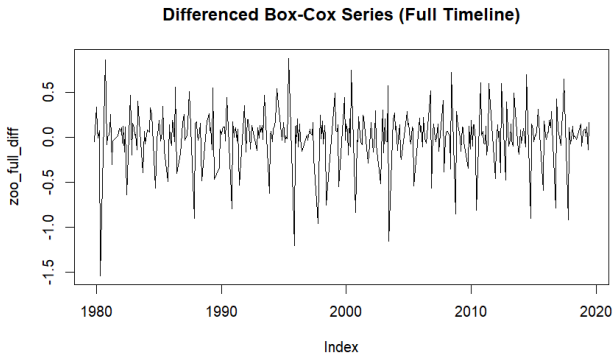

Figure 31: Box-Cox Transformed & Differenced Full Data

```
        Augmented Dickey-Fuller Test

data:  coredata(zoo_full_bc)
Dickey-Fuller = -1.8768, Lag order = 6, p-value = 0.6286
alternative hypothesis: stationary

Warning in adf.test(coredata(na.omit(zoo_full_diff))) :
  p-value smaller than printed p-value

        Augmented Dickey-Fuller Test

data:  coredata(na.omit(zoo_full_diff))
Dickey-Fuller = -11.095, Lag order = 6, p-value = 0.01
alternative hypothesis: stationary
```

Figure 32: ADF Before and After Differencing

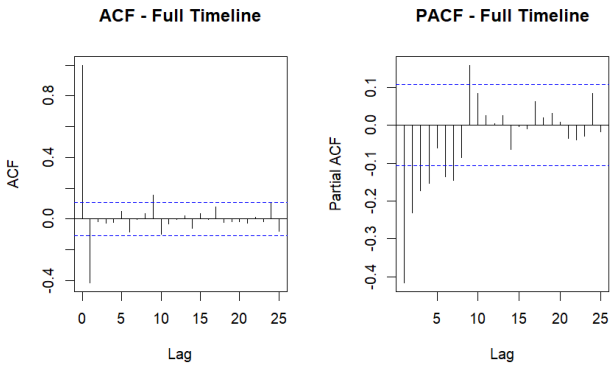

Figure 33: ACF & PACF of Transformed & Differenced Full Data

Fitted Models

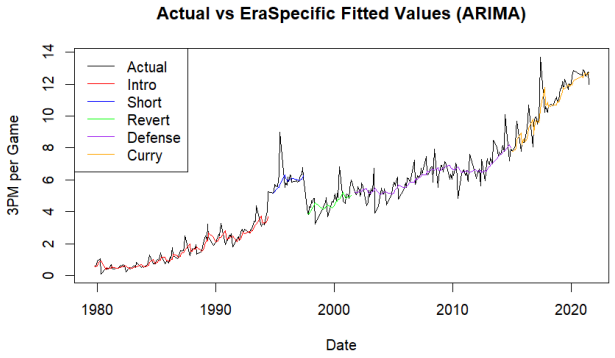

Figure 34: Fitted Models for each Era

Model Summaries

```
Series: ts_curry_tr
ARIMA(0,1,1)

Coefficients:
          ma1
      -0.5748
s.e.   0.1343

sigma^2 = 0.001105:  log likelihood = 81.69
AIC=-159.38   AICc=-159.06   BIC=-155.95

Training set error measures:
                      ME       RMSE        MAE       MPE     MAPE      MASE        ACF1
Training set 0.009741668 0.03244315 0.02207775 0.6176719 1.464607 0.9454176 -0.03850066
```

Figure 35: Model Summary Curry-Only

```
Series: ts_mod_tr
ARIMA(0,1,1) with drift

Coefficients:
          ma1   drift
      -0.8137  0.0127
s.e.   0.0363  0.0029

sigma^2 = 0.04406:  log likelihood = 27.19
AIC=-48.38   AICc=-48.25   BIC=-38.67

Training set error measures:
                      ME      RMSE       MAE        MPE     MAPE      MASE        ACF1
Training set 0.001536773 0.2082334 0.1418874 -0.6251879 5.267182 0.776241 -0.02289785
```

Figure 36: Model Summary Modern Era

```
Series: ts_full_tr
ARIMA(2,1,3) with drift

Coefficients:
         ar1      ar2      ma1     ma2      ma3   drift
      -0.2242  -0.8893  -0.3946  0.7418  -0.6526  0.0151
s.e.   0.0544   0.0573   0.0566  0.0529   0.0436  0.0046

sigma^2 = 0.06541:  log likelihood = -16.18
AIC=46.36   AICc=46.7   BIC=73.1

Training set error measures:
                       ME      RMSE       MAE       MPE     MAPE      MASE        ACF1
Training set 0.0001040251 0.2530823 0.1733954 1.369061 36.83206 0.8804951 0.01403917
```

Figure 37: Model Summary Full Data

Residuals

```
        Ljung-Box test

data:  Residuals from ARIMA(0,1,1)
Q* = 6.9823, df = 7, p-value = 0.4307

Model df: 1.   Total lags used: 8


        Ljung-Box test

data:  Residuals from ARIMA(0,1,1) with drift
Q* = 16.959, df = 9, p-value = 0.04936

Model df: 1.   Total lags used: 10


        Ljung-Box test

data:  Residuals from ARIMA(2,1,3) with drift
Q* = 16.646, df = 5, p-value = 0.005222

Model df: 5.   Total lags used: 10
```

Figure 38: Ljung-Box Test for Residuals for each Segment

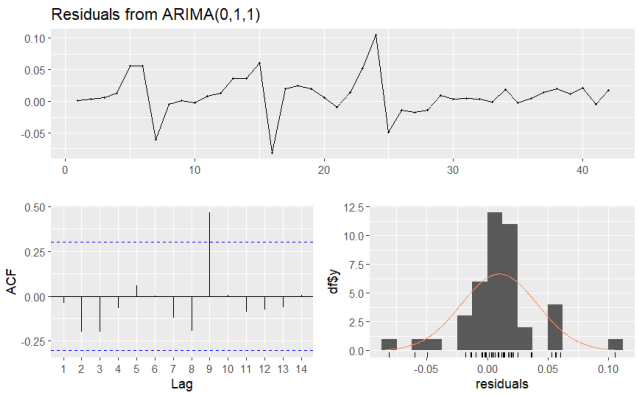

Figure 39: ARIMA Residuals for Curry-Only Segment

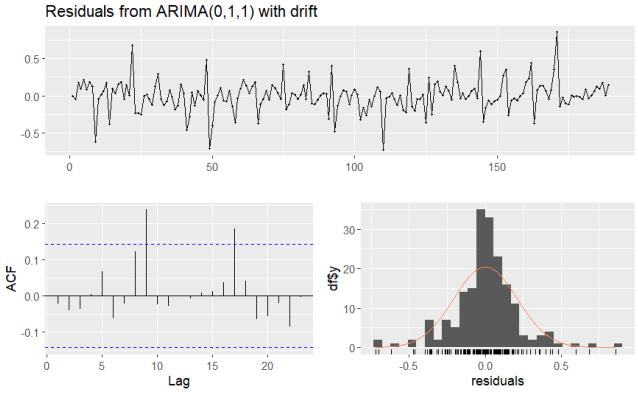

Figure 40: ARIMA Residuals for Modern Era Segment

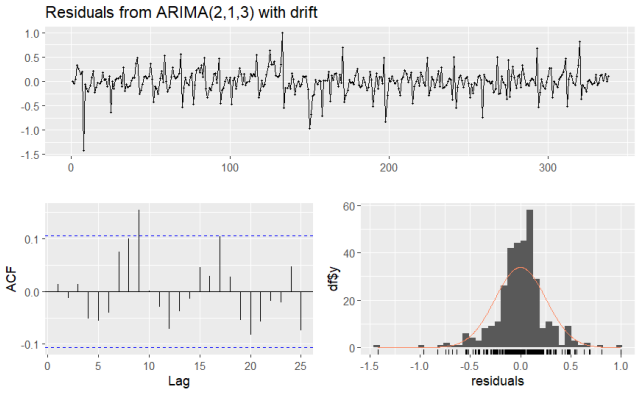

Figure 41: ARIMA Residuals for Full Data